Copper Selenide Nanocrystals for Photothermal Therapy

Colin M. Hessel,[†] Varun Pattani,[‡] Michael Rasch,[†] Matthew Panthani,[†] Bonil Koo,[†] James W. Tunnell,[‡] and Brian A. Korgel[†,]*

[†]Department of Chemical Engineering, Texas Materials Institute, and Center for Nano- and Molecular Science and Technology, [‡]Department of Biomedical Engineering, The University of Texas at Austin; Austin, Texas 78712

*Corresponding author: (T) +1-512-471-5633; (F) +1-512-471-7060; korgel@che.utexas.edu

Supporting information

Experimental Details.

Materials: methanol (Sigma, 99%), ethanol (Sigma, 99%), Poly(isobutylene-alt-maleic anhydride) (Mw~6000 Da, 39 monomer units per molecule, Sigma), anhydrous tetrahydrofuran (Sigma, ≥ 99.9%), anhydrous chloroform (Sigma, ≥ 99 %), sodium hydroxide pellets (Sigma, ≥ 98%), boric acid (Sigma, 99%), copper chloride (anhydrous, beads, ≥ 99.99%), selenourea (ACROS, 99.9+%), oleylamine (Sigma, 70%), 3-aminopropyltrimethoxysilane (Sigma, 97%), ammonium hydroxide (Sigma, 28%, ACS reagent grade), ethanol (Sigma, reagent grade), hydrochloric acid (Sigma, 37%, reagent grade), gold (III) chloride trihydrate (Aldrich, ≥ 99.9%), potassium carbonate (Sigma, ≥99.0%, ACS reagent grade), formaldehyde (Sigma, 37 wt. %, ACS reagent grade), cetyltrimethylammonium bromide (Sigma, ≥ 99%), sodium borohydride (Sigma, 98%), silver nitrate (Sigma, ≥99.0%, ACS reagent grade), ascorbic acid (Sigma, ≥99.0%) and phosphate-buffered saline powder (Sigma) were purchased and used as received. All aqueous solutions were prepared using deionized (DI) water having an 18 MΩ resistance.

$Cu_{2-x}Se$ Nanocrystal Synthesis: All precursor mixtures were prepared in a nitrogen filled glovebox (< 0.1 ppm O_2) and carried out on a greaseless Schlenk line using standard Schlenk techniques. In a typical synthesis the copper and selenium reactant mixtures were prepared in parallel and combined by hot injection to induce nucleation and growth. The copper reactant was prepared by combining 0.198 g (1 mmol) of CuCl and 10 mL of oleylamine in a 125 mL three neck round bottom flask. The mixture was heated to 130 ºC for 10 minutes under nitrogen and vigorous stirring. CuCl dissolved at ~ 90 ºC to form a yellow/blue solution. The solution was cooled to 100 ºC prior to selenium injection. The selenium reactant was prepared by combining 0.123 g (1.0 mmol) of selenourea and 1 mL of oleylamine in a 25 mL 3 neck round bottom flask. The mixture was heated to 200 ºC for 10 min under nitrogen and vigorous stirring. At ~ 170 °C the selenourea dissolved and the solution became dark brown/red. The solution was cooled to 160 ºC, drawn into a syringe, and rapidly injected into the flask containing CuCl and oleylamine. The solution became black upon injection and was heated to 240 ºC for 30 min. The flask was removed from the heating mantle and allowed to cool to room temperature. The nanocrystals were precipitated by the addition of 20 mL, followed by centrifugation at 8000 rpm for 1 min. The blue supernatant was discarded and the green/black nanocrystals were dispersed in anhydrous chloroform. Prior to characterization and polymer coating the dispersions were

centrifuged at 8000 rpm for 5 min to remove aggregated poorly-capped nanocrystals. A typical reaction yields about 100 mg of nanocrystal material.

Gold Nanoshell Synthesis: Gold nanoshells were grown around amine-passivated silica core particles as described in a previous report.[1] In brief, 100 nm diameter colloidal silica spheres (Nissan Chemical Co.) were reacted with 3-aminopropyltrimethoxysilane and NH_4OH in ethanol for 12 hr. The silica spheres were precipitated by centrifugation and dispersed in deionized water titrated to pH 4 with 1 mM HCl. The amine-passivated silica spheres were mixed with an aqueous solution of 2 nm Au nanoparticles to promote Au surface adsorption. The Au-decorated silica spheres were purified from the excess Au nanoparticles by centrifugation and dispersed in deionized water. Au nanoshells were grown by mixing the Au-decorated silica spheres with Au plating solution (0.4 mM $HAuCl_4$ in 1.8 mM K_2CO_3), followed by the addition of 30% formaldehyde solution that served as the reducing agent. The Au nanoshells were collected by centrifugation and dispersed in deionized water. The Au nanoshell thickness was tuned to approximately 10 nm by varying the amount of Au-decorated silica spheres added to the Au plating solution.

Gold Nanorod Synthesis: Gold nanorods passivated with cetyltrimethylammonium bromide (CTAB) were synthesized as previously described.[2] In brief, an aqueous Au nanoparticle seed solution was prepared by reducing $HAuCl_4$ with $NaBH_4$ in the presence of CTAB. The rod growth solution was prepared by combining CTAB, $HAuCl_4$, $AgNO_3$, and ascorbic acid in deionized water. Nanorod growth was initiated by injecting an aliquot of the seed solution into the growth solution, gently mixing for 2-3 seconds, and then storing at 27°C for at least 12 hours. The nanorods were collected by centrifuging to a pellet and then dispersed in deionized water. The nanorods were tuned to 49 × 13 nm (aspect ratio: 3.8) by varying the amounts of $AgNO_3$ or seed solution added to the growth solution.

Commercial Gold Nanorods and Nanoshells: Concentrated Au nanorod and nanoshell solutions were obtained from Nanospectra Biosciences, Inc. (Houston, TX). The fabrication process for both nanoparticles has been discussed in detail previously.[3, 4] The Au nanorods are 23 × 7 nm (aspect ratio: 3.3). The nanoshells are 145 nm in diameter, with an 8 nm thick Au shell. The Au nanorods and nanoshells are conjugated with Polyethylene Glycol.

Amphiphilic Polymer Synthesis: The amphiphilic polymer synthesis was adapted from a published protocol.[27] In a capped, single neck round bottom flask, 100 mL of anhydrous THF, 15 mmol (3.45 mL) of oleylamine, and 3.084 g of poly(isobutylene-alt-maleic anhydride) (20 mmol of monomer units) were added sequentially to form a turbid white solution. The flask was sonicated for 1 min to suspend the insoluble polymer, and was heated at 60 °C for 3 hr under vigorous stirring. The suspension became clear after 15 minutes of stirring. After 3 hours, the solution was cooled to room temperature and reduced in volume to 20 mL with a rotary evaporator. The clear solution was stirred again at 60 °C for 12 hours under vigorous stirring to ensure complete coupling between the polymer and oleylamine. The solution was cooled to room temperature and the remaining solvent was removed with a rotary evaporator, yielding the pale yellow, solid amphiphilic polymer. The solid polymer was transferred to a nitrogen filled glove box (< 0.1 ppm O_2) and dissolved in 25 mL of anhydrous $CHCl_3$ to give a monomer unit

concentration of 0.8 M. The amphiphilic polymer solution was stored in a glass vial within the glovebox until use.

$Cu_{2-x}Se$ Nanocrystal Polymer Coating: The $Cu_{2-x}Se$ nanocrystal polymer coating was adapted from a protocol previously applied to other hydrophobic nanocrystal materials.[5] In a 50 mL round bottom flask, 53 μL of the amphiphilic polymer stock solution (0.8 M monomer units in $CHCl_3$), 0.40 mL of the oleylamine passivated nanocrystals (4.0 mg/mL in anhydrous $CHCl_3$), and 2.55 mL of anhydrous $CHCl_3$ were combined and vortexed with magnetic stirring for 15 minutes at room temperature. The solvent was removed by rotary evaporation to yield a green $Cu_{2-x}Se$-polymer film on the inner wall of the flask. 2.0 mL of aqueous sodium borate buffer (SBB, 50 mM borate, pH 12) was added to the flask and stirred for 15 minutes at room temperature to disperse the $Cu_{2-x}Se$ -polymer. Once suspended, 13.0 mL of DI water was added to the flask to dilute the nanocrystals. The aqueous $Cu_{2-x}Se$ nanocrystal solution was passed through a 0.2 μm-pore syringe filter (Corning, PES membrane), followed by a 0.1 μm-pore syringe filter (Whatman, inorganic membrane). The filtered nanocrystal solution was placed in an ultracentrifugation filter (Amicon Ultra, regenerated cellulose membrane, 50 kDa molecular weight cutoff) and centrifuged at 4000 xg for 4 minutes at room temperature. The colorless filtrate was discarded, and the concentrated nanocrystal retentate solution was diluted to 15.0 mL with aqueous, sterile-filtered phosphate buffered saline (PBS, 150 mM, pH 7.4). The ultracentrifugal filtration process was repeated two more times using PBS to dilute the nanocrystal retentate solution. The nanocrystal solution was dialyzed against PBS at 150 mM and pH 7.4 for 24 hr. The final aqueous nanocrystal solution was stored in a glass vial under ambient conditions until use.

Material Characterization: The $Cu_{2-x}Se$ nanocrystals were examined by low and high resolution transmission electron microscopy (TEM and HRTEM), X-ray diffraction (XRD), and absorbance spectroscopy. TEM images were acquired with either a Phillips EM208 TEM operated at 80 kV accelerating voltage or a JEOL 2010F TEM operated at 200 kV. The nanocrystals were imaged on 200 mesh continuous carbon-coated copper TEM grids (Electron Microscopy Sciences, catalog # CF200-Cu-50), drop-cast from 5 μL of dilute chloroform dispersions of the $Cu_{2-x}Se$ nanocrystals. XRD data was obtained for 5 mg of $Cu_{2-x}Se$ nanocrystals on quartz substrates using a Bruker-Nonius D8 Advance diffractometer. Scans of 2θ° were performed from 10 - 90° in 0.02 (2θ°) increments at a scan rate of 12.0°/minute for 6 hours. Absorbance spectra were acquired either with a Cary 500 UV/vis spectrophotometer or a Beckman Coulter DU720 using a quartz cuvette with a 10 mm optical path length. Zeta potential was measured by laser Doppler anemometry using a Zetasizer Nano ZS instrument (Malvern). Polymer-coated $Cu_{2-x}Se$ nanocrystals dispersed in deionized water ($\sim 10^{16}$ nanocrystals mL^{-1}) were loaded into a disposable folded capillary cell (Malvern, 1.5 mL volume) equipped with two electrodes. The cell was placed in the Zetasizer, which applied an alternating electric field across the cell. Particle mobility in the electric field was measured with the Zetasizer by recording the phase shift of an incident laser beam. Particle mobility was then converted to zeta potential by the Zetasizer software using Smoluchowski theory.[6] The average hydrodynamic diameter of the polymer coated Si nanocrystals in PBS was measured by dynamic light scattering using the Zetasizer instrument. The particles were placed in the disposable capillary cell at $\sim 10^{16}$ nanocrystals mL^{-1} concentration for light scattering measurements. The Zetasizer detected the intensity of backscattered photons at a 173° angle from an incident 4 mW He-Ne (633 nm) laser

over a time interval of 10 seconds, using a sample time (τ) of 0.5 microseconds. The hydrodynamic diameter was then extracted from the light scattering data using the method of cumulants.[7]

Photothermal Heating Experiments: The heating characteristics of all photothermal materials were measured with an infrared camera (FLIR Systems SC4000, Boston, MA), using an 800 nm diode-laser (Opto Power Corp., Tucson, AZ) focused to 6 mm with a biconvex lens as the excitation source. All materials were dispersed in deionized water to an optical density (OD) equal to 1.0 at 800 nm and prior to measurement. Solutions were sonicated for 1 min and 300 μL aliquots were transferred to a 96-well plate. Deionized water was used as the control. The laser power was calibrated to a fluence rate of 2 W/cm^2 with a power meter (Newport Corp., Irvine, CA). Measurements were collected by irradiating each well for 5 min and simultaneously collecting the solution temperature using the infrared camera and ThermoVision software (FLIR Sys., Boston, MA). All comparisons and analyses were performed in MATLAB (The Mathworks Inc., Natick, MA).

Cytotoxicity and In Vitro Studies: Human colorectal carcinoma HCT-116 cells (ATCC, Manassas, VA) were grown in 12-well plates in McCoy's 5A Modified Medium (ATCC) supplemented with fetal bovine serum (10% /volume) (Invitrogen, Carlsbad, CA) and penicillin streptomycin (1% /volume) (Invitrogen). Cells incubated for approximately two days until 80% confluency was reached. After the desired confluency was reached, the medium was removed and the cells rinsed with phosphate buffered saline (PBS) (Thermo Fisher Scientific, Waltham, MA), and charged a combination of new media (0.375 mL) along with a volume of $Cu_{2-x}Se$ dispersion (0.125 mL, 157 mg/L) to give a solution concentration of 39 mg/L (2.8×10^{15} NCs/L, equivalent concentration to 0.25 OD by absorbance spectroscopy). Cells were incubated for 0.5 hr, 1 hr, 3 hr, and 6 hr at 37°C. Control cells received fresh nanoparticle-free supplemented media and were incubated for 6 hours. After the incubation the media was replaced to remove all unbound $Cu_{2-x}Se$ nanocrystals. The cells were exposed to a membrane permeability stain, Trypan blue (Invitrogen), to assess cell death. Dead cells absorb the dye, exhibiting a blue color, whereas viable cells look clear and normal under a brightfield microscope. The cells were incubated for 3 min with Trypan Blue, rinsed with PBS, and quickly imaged. Brightfield images were collected with a brightfield microscope (Carl Zeiss AG Invertoskop D, Germany) equipped with a Powershot G12 camera (Canon Inc, Tokyo, Japan)

In Vitro Photothermal Therapy with $Cu_{2-x}Se$: For the photothermal therapy experiments cells were cultured by the above method by adding $Cu_{2-x}Se$ nanocrystals to the supplemented medium at the equivalent concentration of 0.25 OD. The cells containing $Cu_{2-x}Se$ nanocrystals were incubated 30 min at 37°C. Control cells received fresh nanoparticle-free supplemented medium and were incubated as well for 30 minutes. After incubation the nanoparticle medium was replaced to remove all unbound nanoparticles, and added fresh supplemented medium to the cells. The cells were placed under the infrared camera and irradiated with the NIR diode laser (ThorLabs L808P1WJ, Newton, NJ) for 5 minutes at 30 W/cm^2 and a 1 mm circular spot. The irradiation was performed on both the cells that received the nanoparticle medium as well as the control cells. Cells were incubated for one hr at 37°C to allow any cell death processes to occur. The cells were exposed to the Trypan Blue by the same method as above to observe cell death.

All imaging was performed with a brightfield microscope equipped with a Canon Powershot G12.

Additional X-ray diffraction data on $Cu_{2-x}Se$ nanocrystals obtained from various reactions

Figure S1 shows a collection of XRD data obtained from $Cu_{2-x}Se$ nanocrystals made under a variety of reaction conditions. Table S1 summarizes the different reaction conditions used, corresponding to the samples in Figure S1.

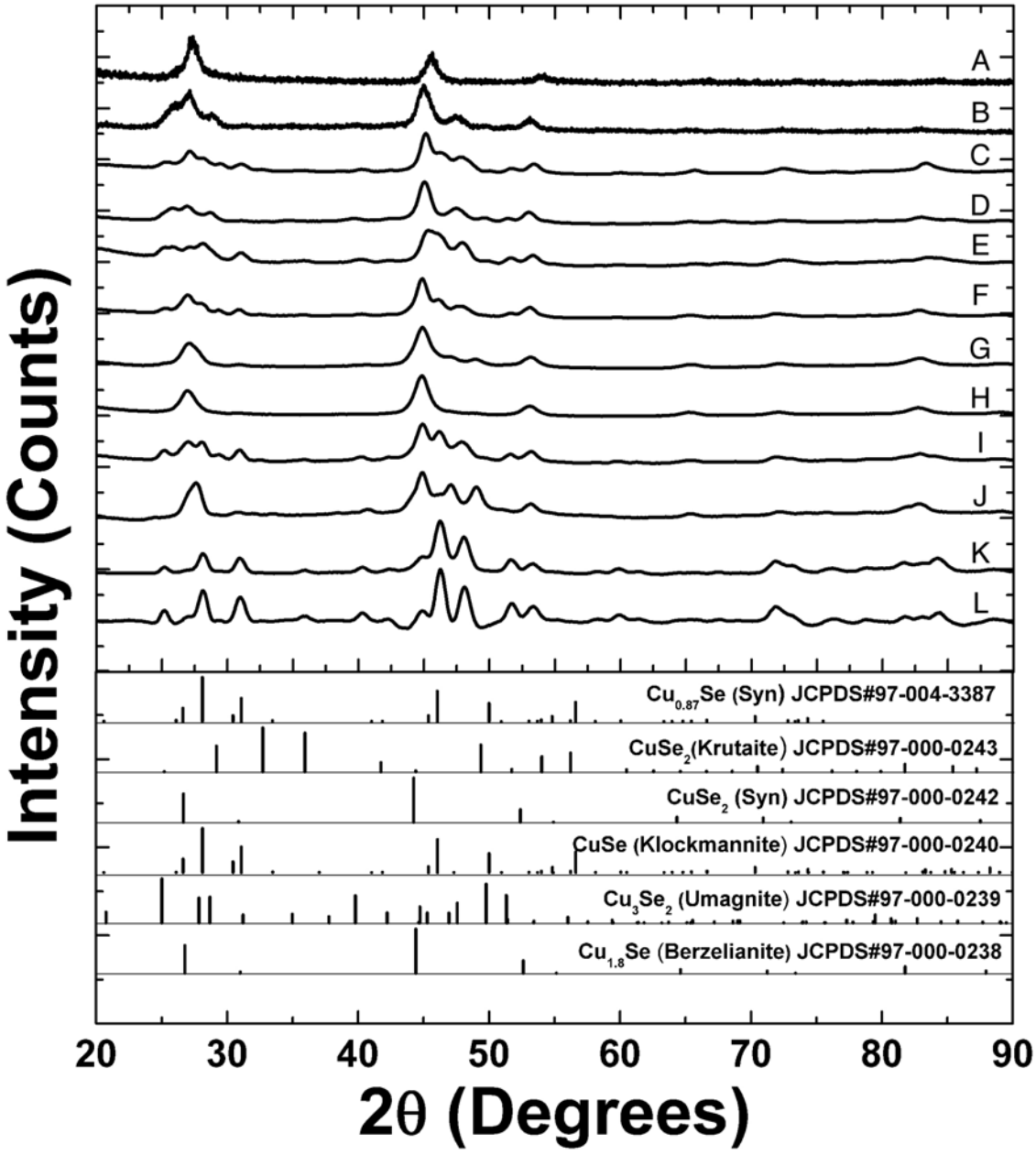

Figure S1: XRD patterns for $Cu_{2-x}Se$ nanocrystals synthesized using different reaction times, solvent purity and temperature. The synthetic conditions corresponding to each curve are

provided in Table S1. The XRD peak positions for various phases of copper selenide are included for reference.

Table S1: Reaction conditions, solvent purity, nanocrystal size and morphology, and absorbance peak maxima for a series of copper selenide reactions. Figure S1 shows the corresponding XRD data for each reaction.

reaction	reaction time (min)	reaction temperature (°C)	solvent purity	morphology	size (nm)	absorbance maximum (nm)
A	30	220	99.97	sphere	12	1000
B	30	220	99.97	sphere	12	1000
C	60	240	99.97	sphere	12	1100
D	30	240	99.97	sphere	12	1050
E	30	240	99.7	poor quality	na	1100
F	15	240	98	poor quality	na	1150
G	30	240	98	sphere	14	1200
H	30	240	98	disc	10	1250
I	90	240	98	disc, sphere	12	1250
J	60	240	98	disc, sphere	13	1100
K	30	240	98	poor quality	10	1250
L	60	240	99.9	sphere, triangle	11	1050

Calculation of the molar extinction coefficient

The molar extinction coefficient of $Cu_{2-x}Se$ nanocrystals was determined by linearly fitting the extinction maxima for various nanocrystal solutions to the Beer Lambert Law,

$$A(\lambda) = \varepsilon LC \tag{S1}$$

where A is the absorbance at a wavelength λ, ε is the molar extinction coefficient, L is the pathlength (1 cm), and C is the concentration of nanocrystals (in L g^{-1} cm^{-1}). The extinction coefficient was determined by plotting the slope (in L g^{-1} cm^{-1}) of each linear fit against wavelength. Figure S2 shows absorbance spectra for the $Cu_{2-x}Se$ nanocrystals measured for a variety of nanocrystal concentrations. Figure S3 shows linear fits of Eqn (S1) to the absorbance at various wavelengths as an example of how the molar extinction coefficients were determined.

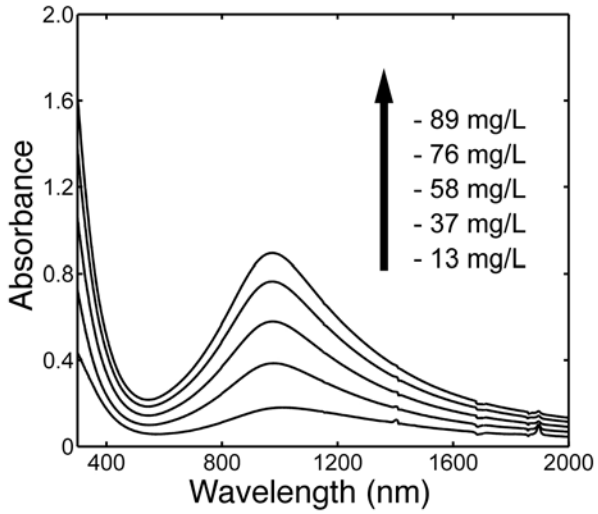

Figure S2: Room temperature UV-vis-NIR absorbance spectra for $Cu_{2-x}Se$ nancrystals dispersed in toluene at various solution concentrations to determine the $Cu_{2-x}Se$ nanocrystal molar extinction coefficient.

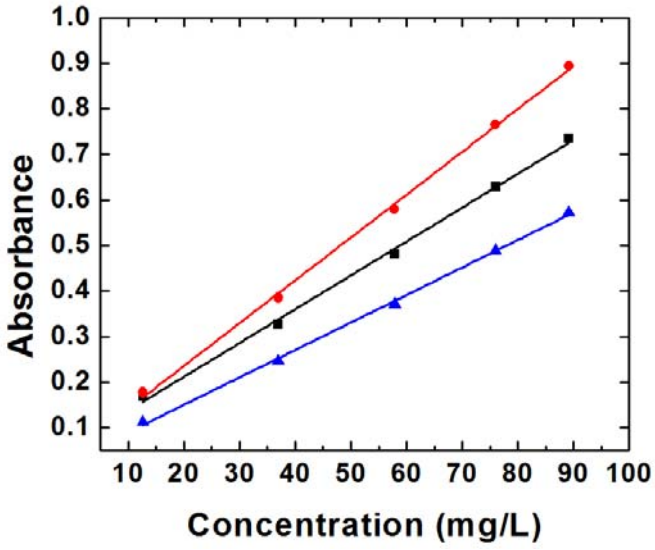

Figure S3: Plots of linear fits to extinction vs. wavelength for $Cu_{2-x}Se$ solutions at 800 nm (blue triangle), 1100 nm (black square), and 970 nm (red circle).

Since the molar absorption coefficient is dependent on the physical mass of the material, the experimentally calculated absorption coefficient contains mass contributions from both the nanocrystals and surface bound oleylamine ligands. The mass contribution from oleyamine was found to be 9% by thermogravimetric analysis (TGA) (Figure S4). This value matched quite well with the theoretical estimate of 12%, which was calculated by determining the surface coverage of oleylamine on the $Cu_{2-x}Se$ nanocrystal surface.

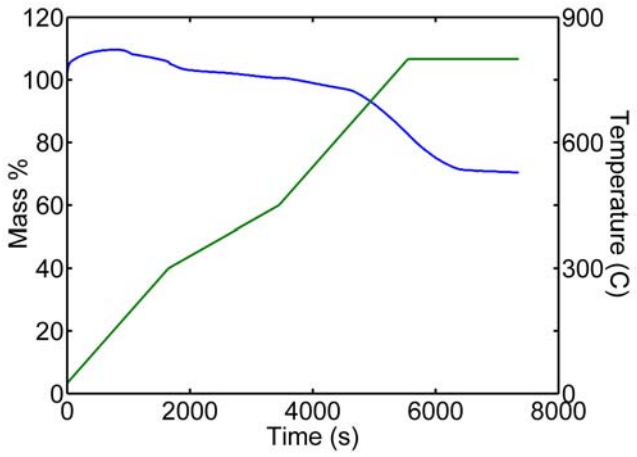

Figure S4: Thermogravimetric analysis (TGA) of oleylamine-coated $Cu_{2-x}Se$ nanocrystals performed under nitrogen atmosphere.

The surface coverage of the ligand was estimated by modeling the $Cu_{2-x}Se$ nanocrystal surface as a sheet, and dividing by the footprint of cylindrical oleylamine ligands. The surface area of one oleyamine ligand is:

$$L \approx (0.154\,nm + 0.1265\,nm \times 18) = 2.431\,nm$$
$$V \approx (27.4\,nm + 26.9\,nm \times 18)/1000 = 0.512\,nm^3$$
$$A = \frac{V}{L} = \frac{0.512\,nm^3}{2.431\,nm} = 0.21\,nm^2$$

The mass fraction of the oleylamine per 16 nm nanocrystal (measured by TEM) is then:

$$m_{CuSe} = \frac{4}{3}\pi r^3 \times \rho_{CuSe} = \frac{4}{3}\pi(8\,nm)^3 \times 5.8\,g/cm^3 = 1.2 \times 10^{-17}\,g\,CuSe/Nanocrystal$$
$$m_{Oleyla\,min\,e} = 4\pi r^2 \times \left(\frac{MW_{oleyla\,min\,e}}{A \times 6.022 \times 10^{23}}\right)$$
$$= 4\pi 8\,nm^2 \times \left(\frac{267.5\,g/mol}{0.21\,nm^2 \times 6.022 \times 10^{23}}\right) = 1.7 \times 10^{-18}\,g\,oleyla\,min\,e/nanocrystal$$
$$\frac{m_{oleyla\,min\,e}}{m_{CuSe} + m_{oleyla\,min\,e}} = \frac{1.7 \times 10^{-18}\,g}{1.2 \times 10^{-17} + 1.7 \times 10^{-18}\,g} = 0.124\ or\ 12.4\%$$

Using the true $Cu_{2-x}Se$ mass, the molar extinction coefficient is calculated by:

$$\varepsilon(L\,mol^{-1}cm^{-1}) = \varepsilon(L\,g^{-1}cm^{-1}) \times \left(\frac{1\,g\ Nanocrystals}{0.90\,g\ CuSe}\right) \times \left(\frac{1.2 \times 10^{-17}\,g\,CuSe}{Nanocrystal}\right) \times \left(\frac{6.022 \times 10^{23}\,nanocrystals}{mol}\right)$$

This gives the spectrum in Figure 3.

Summary of heat transfer coefficients used to determine the photothermal transduction efficiency.

Table S2 summarizes the thermal time constants measured and used to calculate the photothermal transduction efficiencies of the $Cu_{2-x}Se$ nanocrystals and the Au nanorods and nanoshells.

Table S2: Thermal time constants and heat transfer coefficients for $Cu_{2-x}Se$, Au nanorods and Au nanoshells determined from steady state solution heating and cooling curves shown in Figure 6A.

Material	Thermal time constant (s) - heating	Thermal time constant (s) - cooling	Heat transfer coefficient (mW/C) - heating	Heat transfer coefficient (mW/C) - cooling
$Cu_{2-x}Se$	331.56	320.82	3.866	3.668
Au nanorods	357.27	376.65	4.141	3.389
Au nanoshells	333.56	407.66	4.166	4.306

References

1. Rasch, M. R.; Sokolov, K. V.; Korgel, B. A. *Langmuir* **2009,** *25*, 11777-11785.
2. Smith, D. K.; Miller, N. R.; Korgel, B. A. *Langmuir* **2009,** *25*, 9518-9524.
3. Oldenburg, S. J.; Averitt, R. D.; Westcott, S. L.; Halas, N. J. *Chem. Phys. Lett.* **1998,** *288*, 243-247.
4. Jana, N. R.; Gearheart, L.; Murphy, C. J. *J. Phys. Chem. B* **2001,** *105*, 4065-4067.
5. Lin, C. A. J.; Sperling, R. A.; Li, J. K.; Yang, T. Y.; Li, P. Y.; Zanella, M.; Chang, W. H.; Parak, W. J. *Small* **2008,** *4*, 334-341.
6. Smoluchowski, M. V. *Bull. Int. Acad. Sci. Cracovie* **1903,** *184*.
7. Frisken, B. J. *Appl. Opt.* **2001,** *40*, 4087-4091.